

Measuring nontrivial fusion rule of Majorana fermions in inhomogeneous transverse Ising chain

Yin-Chen He¹, and Yan Chen^{1,2}

¹*Department of Physics, State Key Laboratory of Surface Physics and Laboratory of Advanced Materials, Fudan University, Shanghai 200433, China*
²*Department of Physics and Center of Theoretical and Computational Physics, The University of Hong Kong, Pokfulam Road, Hong Kong, China*

We describe various dynamical processes aimed to create and fuse Majorana fermions in an inhomogeneous Kitaev's wire. We show that, with the undesired excitations suppressed by inhomogeneity, fusion of Majorana fermions will result in universal measurable excitations, which can serve as a direct verification of Majorana fermions fusion rule. Moreover, we design a protocol to detect the oscillatory tunneling between two unpaired Majorana fermions. Most remarkably, our proposal is valid for transverse Ising chain, which provides a promising way to test nontrivial properties of Majorana fermions experimentally.

PACS numbers: 03.65.Vf, 74.40.Gh, 71.10.Pm, 67.85.-d

Majorana fermions (MFs) are self-conjugate quasiparticles ($\gamma^\dagger = \gamma$) [1], and non-Abelian anyons obeying exotic braiding statistics and fusion rule [2, 3]. Recent years have seen much excitement over MFs, not only because of their peculiar properties, but also due to possible applications for topological quantum computation [4]. Creating, manipulating and detecting MFs experimentally remains a great challenge, although many theoretical schemes for that have been proposed [5–15]. As far as their realization is concerned, an encouraging progress has been made for one dimensional systems, especially for semiconducting wires [16], where a zero-bias conductance peak (ZBCP) [17] and a fractional Josephson effect [10, 18] have been recently measured [19, 20]. However, it still remains controversial whether the ZBCP arises from the MFs [21] and the fractional Josephson effect can also be observed in non-topological superconductor junctions [22]. Hence up to now we lack such evidence for MFs, which would unambiguously and straightforwardly demonstrate their fusion rules and braiding statistics.

Experiments in quantum simulation offer a promising platform to study and mimic many physical systems from condensed matter to cosmology [23]. The theory suggests that with a spin-orbital coupling in ultracold atoms, one can realize topological superfluids [8] as well as Kitaev's wire [24]. However, these theoretical proposals are still hard to implement experimentally. On the other hand, transverse Ising chain model (TIM) presents itself as a system which is easy to realize and to control in quantum simulation experiments. It has been realized in a large variety of experimental systems, including ultracold atoms [25], trapped ions [26], and Josephson circuits [27]. TIM is related to Kitaev's wire by a non-local Jordan-Wigner transformation. The danger is, however, that such non-local transformation may render MFs obscure.

In this Letter, we show that one can verify MFs fusion rule by measuring non-equilibrium dynamics of an inho-

ogeneous TIM chain. In particular, we discuss non-equilibrium dynamics in Kitaev's wire, involving creating, manipulating and fusing MFs. We introduce an inhomogeneity in the system, which helps to suppress undesired excitations and to manipulate the MFs. We highlight that the fusion of MFs would give rise to a promising result in TIM chain, an emergence of universal number of excitations. The universal emergent excitations may serve as a touchstone of nontrivial fusion rule of MFs. We also find that oscillatory tunneling between unpaired MFs may show up and can be measured via oscillatory number of emergent excitations.

The Hamiltonian and its features.— In the following, we consider an open TIM chain with an inhomogeneous magnetic field. The Hamiltonian can be expressed as

$$H_T = - \sum_{i=1}^N h_i \sigma_i^z - J \sum_{i=1}^{N-1} \sigma_i^x \sigma_{i+1}^x. \quad (1)$$

The Jordan-Wigner transformation: $\sigma_i^z = 2c_i^\dagger c_i - 1$ and $\sigma_i^x = \prod_{j=1}^{i-1} \sigma_j^z (c_i^\dagger + c_i)$, maps TIM into Kitaev's p-wave superconducting wire model:

$$H = - \sum_{j=1}^N h_j (2c_j^\dagger c_j - 1) - \sum_{j=1}^{N-1} J (c_j - c_j^\dagger)(c_{j+1} + c_{j+1}^\dagger) \quad (2)$$

where c_j denotes spinless fermion operator, h_j can be considered as a site dependent chemical potential.

For TIM, the ground state is doubly-degenerate ferromagnetic state when $|h_i| \ll J$. For the opposite limit $|h_i| \gg J$, the chain will be in the spin polarized state with all spins oriented along the magnetic field. The two phases are separated by the quantum critical point (QCP); for the homogeneous case $h_j = h$, QCP is at $|h| = J$. Correspondingly, when $|h| < J$, the Kitaev's wire is in a topological phase, which has two zero energy MFs located on the both ends. The existence of MFs can be easily understood by considering

the limiting case $h = 0$. Expressing the fermion operator $c_j = (\gamma_{2j-1} + i\gamma_{2j})/2$ with MF operator, which satisfies $\gamma_s^\dagger = \gamma_s$ and $\{\gamma_s, \gamma_t\} = 2\delta_{st}$, one obtains $H = -iJ \sum_{j=1}^{N-1} \gamma_{2j} \gamma_{2j+1}$. Recombining the MF operator into fermion operator $\tilde{c}_j = (\gamma_{2j} + i\gamma_{2j+1})/2$, the Hamiltonian becomes $H = -J \sum_{j=1}^{N-1} (2\tilde{c}_j^\dagger \tilde{c}_j - 1)$. Therefore, the groundstate of the chain is a quantum state with all \tilde{c}_j fermions occupied, and with two unpaired MFs γ_1 and γ_{2N} localized at both ends. For two unpaired MFs, they obey the MFs fusion rule, fusing into a superposition of the vacuum state 0 and one fermion c [4]:

$$\gamma \times \gamma = 0 + c. \quad (3)$$

Verifying the fusion rule of MFs comprises two steps: 1) creating two unpaired MFs, 2) measuring the fused state. Even though MFs are created in pairs, one can still have two MFs from different pairs, which are unpaired and satisfy the MFs fusion rule in Eq. (3).

Inhomogeneous potential.— For a topological phase with well defined MFs, two fused MFs may enter either into vacuum or into one fermion state. Since both are the groundstates of the system, it is hard to distinguish them. To measure the fused state more transparently, one may drive the system across the QCP to a non-topological phase, where the one fermion state becomes an excitation, making it easier to be differentiated from the vacuum state. However, the vanishing energy gap and divergent relaxation time at QCP will inevitably create many excitations, whose density is determined by the Kibble-Zurek mechanism (KZM) [28, 29]. For instance, imposing a linear quench $h = -J + t/t_Q$ from $t < 0$ to $t > 0$, will produce excitations whose number n by the usual KZ mechanism scales as $n \propto Nt_Q^{-1/2}$ [29]. These excitations will obscure the MFs fused excitation.

In order to measure the fusion excitation of MFs more effectively, one needs to suppress the KZM excitations. An intuitive way is to do the experiment in a system of small size. For a system with size L , the minimum gap is proportional to $1/L$, and KZM excitations may vanish if the quench process is sufficiently slow. However, the smaller the system the greater is the overlap between the MFs located at its opposite ends, making their measurement impossible. An alternative way to suppress KZM excitations is to consider an inhomogeneous system [30]. This physical result can be understood qualitatively as follows: when an inhomogeneous system undergoes a quench process, the critical point will be crossed locally and the MF associated with boundary between the topological and non-topological phases will shift as the quench process goes on. It is important that the energy spectrum of the bulk of the inhomogeneous system always has finite gap during the quench process. Consequently, the inhomogeneous setup not only suppresses the bulk KZM excitations but also helps one to manipulate the MFs.

Numerical simulations.— First we consider two simple

quench processes, where the chemical potential is inhomogeneous and varies with time:

$$\text{Process I: } h_n(t) = \alpha^2 n^2 + h_0 + t/t_Q \quad (4)$$

$$\text{Process II: } h_n(t) = \alpha^2 (n - N/2 - 1/2)^2 + h_0 + t/t_Q$$

where α denotes the coefficient of parabolic confining potential. Here we choose the system size $N = 100$. With an increase of α , the minimum gap during the whole adiabatic quench process also increases, making it easier to suppress the KZM excitations. The term t/t_Q in (4) represents the quench, with t_Q being the quench time, which determines the rate of change of the chemical potential. During the two quench processes, the chemical potential will be ramped from $h_n < -J$ to $h_n > J$. Using the Bogoliubov transformation $a_m^\dagger = \sum_n (u_{nm} c_n^\dagger + v_{nm} c_n)$, we can diagonalize the Hamiltonian for any given time, and find that for both quench processes there is always an energy gap [31].

To study the non-equilibrium dynamics, we consider the BCS groundstate of the chain $|\psi\rangle = \prod_i a_i^\dagger |0\rangle / N_0$, and the state after the evolution is $|\psi_f\rangle = \prod_i a_i^\dagger(t_f) |0\rangle / N_0$ with

$$\hat{a}_m^\dagger(t_f) = U \hat{a}_m^\dagger U^\dagger, \quad U = T \left\{ \exp \left[-i \int_{t_0}^{t_f} H(t) dt \right] \right\} \quad (5)$$

where N_0 is normalization constant, $U(t)$ is time evolution operator, T is time ordering operator. We also diagonalize the final Hamiltonian $H(t_f) = \sum_m (E_m b_m^\dagger b_m - E_m b_m b_m^\dagger)$, with $E_m < 0$. Then the number of excitations can be written as

$$n_{ex} = \sum_m \langle \psi_f | b_m b_m^\dagger | \psi_f \rangle. \quad (6)$$

Fig. 1(a)-(b) illustrate the number of excitations for two quench processes, respectively. It is clear that KZM excitations will be greatly suppressed for long quench time t_Q . In particular, process I gives rise to no excitations while process II yields excitations with universal number 1. To further understand the above numerical results, we should carefully consider the two quench processes. In quench process I, the chain is prepared in a topologically trivial phase (Fig. 1(c)-I). Then by gradually increasing the chemical potential, we create two MFs by pulling them out of the vacuum at the right end of the system (Fig. 1(c)-II). As the quench goes on, the two MFs will separate initially (Fig. 1(c)-III), then approach each other (Fig. 1(c)-IV), and finally fuse at the left end (Fig. 1(c)-V). The whole process only involves two paired MFs, no matter how they move they will always fuse into the vacuum, yielding no excitations. This process can't be used to detect MFs fusion rule, but it can serve as an adiabatic way to evolve the whole chain into different quantum phase.

In the quench process II four MFs participate. As depicted in Fig. 1(d)-II, two pairs of MFs, (γ_1, γ_2) and

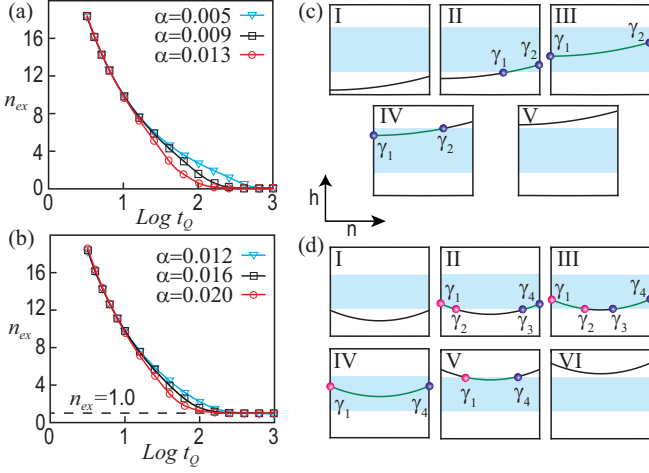


FIG. 1. The number of excitations after the quench process I (a) and II (b). A cartoon picture for the two quench processes I (c) and II (d). Topological phase regions are marked in light cyan. MFs with the same color, (γ_1, γ_2) and (γ_3, γ_4) , are paired MFs, which will fuse into the vacuum state. Here we choose $J = 1$.

(γ_3, γ_4) , are pulled out of the vacuum on both ends. When the potential is further increased, two unpaired MFs, γ_2 and γ_3 , may fuse at the potential center (Fig. 1(d)-III to IV), into a superposition of the vacuum $|0\rangle$ and one fermion $|1\rangle$, as shown in Eq. (3). Then the quantum state can be written as $(|0\rangle|0'\rangle + |1\rangle|1'\rangle)/\sqrt{2}$, where $|0\rangle$ and $|1\rangle$ refers to the fusion state of γ_1 and γ_4 to be vacuum or a fermion. When the whole chain is in the topological phase (Fig. 1(d)-IV), only $|1'\rangle$ is an excited state, then $n_{ex} = 0.5$. Similarly, when the whole chain is ramped non-topological (Fig. 1(d)-VI), both $|1\rangle$ and $|1'\rangle$ are excited states, thus $n_{ex} = 1$. This universal single excitation is a direct consequence of the MFs fusion rule.

Measuring MFs fusion rule in TIM.— The groundstate of TIM is a BCS type state with all eigenstates of the Bogoliubov quasiparticles filled, thus the excitation number created by the quench process is the same as Eq. (6). However, due to the quantum fluctuations, the excitation in TIM is usually a highly entangled superposition of many spin configurations, which is difficult to detect experimentally by local measurements.

To clarify the excitations in TIM unambiguously, one may tune the system parameters to two limiting cases: $h_i = 0$ or $J = 0$. At $h_i = 0$, the groundstate of TIM is just an exact ferromagnetic state with spin-spin correlations of nearest neighbors: $\langle \sigma_j^x \sigma_{j+1}^x \rangle = 1$. An excitation, the domain wall, is located on the bond $\langle j, j+1 \rangle$ with $\langle \sigma_j^x \sigma_{j+1}^x \rangle = -1$. When $J = 0$, the groundstate of TIM is an exact paramagnetic state with spins aligned parallel to the magnetic field, and the excitation is a flipped spin. In the quench process II, after fusing γ_2 and γ_3 (Fig. 1(d)-IV), the corresponding TIM chain is in the

ferromagnetic phase. Then one tunes slowly the magnetic field to 0, and measures the spin-spin correlation $\langle \sum_i \sigma_i^x \sigma_{i+1}^x \rangle$, one may obtain $\langle \sum_{i=1}^{N-1} \sigma_i^x \sigma_{i+1}^x \rangle = N - 2$, signifying the emergence of 0.5 excitation. Similarly, after the fusion of γ_1 and γ_4 (Fig. 1(d)-VI), the corresponding TIM chain is in a paramagnetic phase. Then one tunes slowly the spin-spin coupling J to 0, and measures the magnetization along the z direction, one may have $\langle \sum_{i=1}^N \sigma_i^z \rangle = N - 2$, signifying the emergence of 1 excitation. Thus, the universal fusion excitation of MFs can be measured in TIM. However, the emergent excitation here is not well localized in real space [31], which is inconvenient for experimental detection.

To facilitate a detection of the MFs fusion rule, we design a quench process III (shown schematically in Fig. 2(a)), which requires more delicate control on potential but the emergent excitations in TIM becomes perfectly trapped, as illustrated in Fig. 2(b). Initially we prepare a topological trivial phase with the potential monotonically increasing along the chain (Fig. 2(a)-I), and then slowly increase the potential so that the whole chain enters into the topological phase with two paired MFs (γ_1, γ_2) appearing at the both ends (Fig. 2(a)-II). This process must be adiabatic as was discussed for the quench process I. Then we adiabatically change the potential to be harmonically distributed (Fig. 2(a)-III). After that, we decrease the potential, creating two paired MFs (γ_3, γ_4) at the center (Fig. 2(a)-IV). Finally, γ_1 and γ_3 fuse at the left end, γ_2 and γ_4 may fuse at the right end (Fig. 2(a)-V to VI). This process III is similar as process II, where we fuse two unpaired MFs, nevertheless, our numerical calculation show that in a remarkable way the fused excitations (flipped spins) are perfectly trapped at the both ends of the system [31].

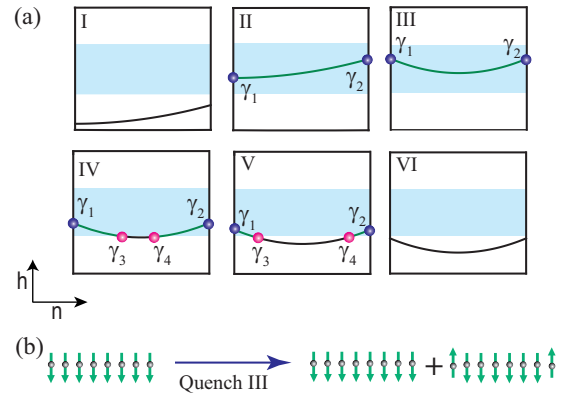


FIG. 2. (a) The quench process III. The topological phase regions are marked in light cyan. The MFs with same color, (γ_1, γ_2) and (γ_3, γ_4) , are paired MFs, which will fuse into the vacuum state. (b) A schematic state evolution of the quench process. Initial state (groundstate): all spins pointing in the $-z$ direction. The final state: an equal-weighted superposition of the groundstate and excited state with two end spins flipped into the z direction.

Oscillatory tunneling of unpaired MFs.— When two MFs (γ_a, γ_b) become close so that the interaction between them is significant, $H' = -iA\gamma_a\gamma_b$, this can be approximated as a time evolution process with a time evolution operator $U = \exp(-iH't)$. For two paired MFs, denoted as $\gamma_1 - i\gamma_2$, the time evolution only gives a phase factor, $U(\gamma_1 - i\gamma_2)U^\dagger = \exp(i2At)(\gamma_1 - i\gamma_2)$. For two unpaired MFs (γ_2, γ_3), the situation is quite different. We suppose that γ_2 is paired with γ_1 and γ_3 is paired with γ_4 . Then the state under the time evolution becomes

$$\begin{aligned} U(\gamma_1 - i\gamma_2)U^\dagger &= \gamma_1 - i\cos(2At)\gamma_2 - i\sin(2At)\gamma_3, \\ U(\gamma_4 - i\gamma_3)U^\dagger &= \gamma_4 - i\cos(2At)\gamma_3 + i\sin(2At)\gamma_2. \end{aligned} \quad (7)$$

Therefore, for two unpaired MFs within a finite range, there will be oscillatory tunneling between them.

In fact, we can design a process IV to measure such oscillatory tunneling between two unpaired MFs. The process IV is similar to the process II plotted in Fig. 1(d). However, here we only ramp the chain from Fig. 1(d)-I to Fig. 1(d)-III, and pause at Fig. 1(d)-III. The MFs γ_2 and γ_3 are separated by l lattice spacings, having a finite coupling $-iA(l)\gamma_2\gamma_3$ between them [32]. Then we let the system evolve for certain time duration t_e , such that γ_2 and γ_3 will tunnel to each other, with the resulting states $\tilde{\gamma}_2 = \cos[2A(l)t_e]\gamma_2 + \sin[2A(l)t_e]\gamma_3$ and $\tilde{\gamma}_3 = \cos[2A(l)t_e]\gamma_3 - \sin[2A(l)t_e]\gamma_2$. After that, we slowly drive the chain back from Fig. 1(d)-III to Fig. 1(d)-I, where we will fuse $(\gamma_1, \tilde{\gamma}_2)$ and $(\tilde{\gamma}_3, \gamma_4)$ at the left and right ends. The fused excitations can be easily measured in TIM, since they will be perfectly localized at the edges of the chain, similar to Fig. 3(a). One can obtain that the number of excitations created by the whole process:

$$n_{ex} = 1 - \cos[2A(l)t_e + \varphi_0] \quad (8)$$

The phase factor φ_0 comes from the fact that, when two unpaired MFs approach and separate with each other, the tunneling between them yields a nonuniversal phase factor (φ_0). This phase factor is difficult to determine analytically. However, in experiment one can make the process (from Fig. 1(d)-I to III as well as from Fig. 1(d)-III to I) identical, then phase φ_0 will be the same for the quench processes with different time duration t_e . In Fig. 3(b), we plot numerical results for the excitation number created by such process IV, which clearly shows sinusoidal oscillations. The oscillation period of n_{ex} is determined by $\tau = \pi/A(l)$, with which we can calculate the two MFs coupling strength $A(l)$, as shown in Fig. 3(c). We find that $\ln A(l)$ can be well fitted by a quadratic function.

Braiding MFs through T-junctions in TIM.— It has been shown that one can use T-junctions in Kitaev's wire to implement braiding operations of MFs [3]. However, T-junctions design for TIM will fail to detect the braiding statistics of MFs, since the model with T-junctions is

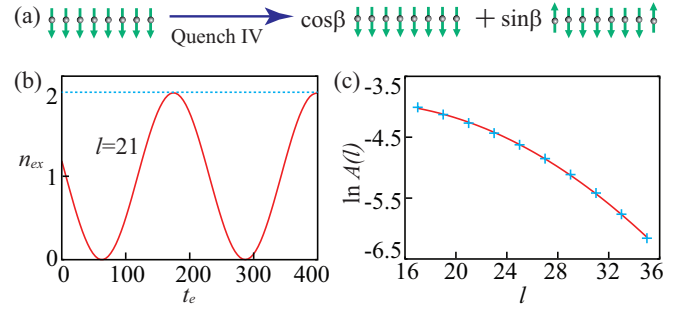


FIG. 3. (a) A schematic state evolution of the quench process IV. Initial state (groundstate): all spins pointing in the $-z$ direction. The final state: a superposition of the groundstate and excited state with two end spins flipped into the z direction. Here $\beta = At_e + \varphi_0/2$. (b) The oscillation of excitation number as a function of duration time t_e . (c) The coupling strength $A(l)$ between two unpaired MFs as a function of distance l . We take the following parameters, $\alpha = 0.02$ and $J = 1$.

not one-dimensional and so the Jordan-Wigner transformation does not map it to a fermion model with a local Hamiltonian.

Experimental realization.— Up to now, several experimental systems may become candidates to test our theoretical proposal. One promising approach is to simulate TIM using ultracold atoms on optical lattice, where TIM with additional magnetic field in the x direction has already been constructed [33]. Moreover, the technique for single site measurement in ultracold atoms becomes available [34]. On the other hand, TIM has been successfully simulated in the trapped ions system, though with only a small number ($n \sim 8$) of spins [26, 35]. A recent work [36], which has hundreds of spins with variable-range spin-spin Ising-type interactions simulated, pave new way on large-scale quantum simulations for TIM. Another way to simulate spin chain models is to use Josephson superconducting circuits. A decoherence time as long as 0.1ms has been achieved in Josephson circuits which is sufficient to test our theoretical predictions [37].

Summary.— We have studied quench dynamics of Kitaev's wire under the inhomogeneous potential. We propose and numerically confirm that, with an inhomogeneous structure of the quench, the fusion rule of MFs can be unambiguously detected with a remarkable suppression of the KZM excitations. The fusion of MFs will result in universal excitations, which may serve as a direct evidence of the MFs fusion rule. We also find that oscillatory tunneling between two unpaired MFs will create excitations whose number oscillates with the time of evolution. We show that in TIM one can measure both universal and oscillatory emergent excitations. Our theoretical proposal provides a promising way to verify the nontrivial properties of MFs experimentally in ultracold atoms, trapped ions or Josephson junctions.

We acknowledge J.Q. You and Y. Yu for useful discussions. Y.-C. He appreciates the help of Y.-Y. Zhao, K. Ding and J.-D. Zang. This work was supported by the National Natural Science Foundation of China (Grant Nos. 11074043 and 11274069) and the State Key Programs of China (Grant Nos. 2009CB929204 and 2012CB921604) and Shanghai Municipal Government, the RGC grants in HKSAR.

-
- [1] E. Majorana, *Nuovo Cimento* **14**, 171 (1937).
 - [2] D. A. Ivanov, *Phys. Rev. Lett.* **86**, 268 (2001).
 - [3] J. Alicea, Y. Oreg, G. Refael, F. von Oppen, and M. P. A. Fisher, *Nature Phys.* **7**, 412 (2011).
 - [4] C. Nayak, S. H. Simon, A. Stern, M. Freedman, and S. Das Sarma, *Rev. Mod. Phys.* **80**, 1083 (2008).
 - [5] G. Moore and N. Read, *Nucl. Phys. B* **360**, 362 (1991).
 - [6] N. Read and D. Green, *Phys. Rev. B* **61**, 10267 (2000).
 - [7] L. Fu and C. L. Kane, *Phys. Rev. Lett.* **100**, 096407 (2008).
 - [8] M. Sato, Y. Takahashi, and S. Fujimoto, *Phys. Rev. Lett.* **103**, 020401 (2009).
 - [9] A. Kitaev, *Ann. Phys. (N.Y.)* **321**, 2 (2006).
 - [10] A. Y. Kitaev, *Physics-Uspekhi* **44**, 131 (2001).
 - [11] C. J. Bolech and E. Demler, *Phys. Rev. Lett.* **98**, 237002 (2007).
 - [12] S. Tewari, C. Zhang, S. Das Sarma, C. Nayak, and D.-H. Lee, *Phys. Rev. Lett.* **100**, 027001 (2008).
 - [13] Y. Tanaka, T. Yokoyama, and N. Nagaosa, *Phys. Rev. Lett.* **103**, 107002 (2009).
 - [14] K. T. Law, P. A. Lee, and T. K. Ng, *Phys. Rev. Lett.* **103**, 237001 (2009).
 - [15] A. R. Akhmerov, J. Nilsson, and C. W. J. Beenakker, *Phys. Rev. Lett.* **102**, 216404 (2009).
 - [16] J. D. Sau, R. M. Lutchyn, S. Tewari, and S. Das Sarma, *Phys. Rev. Lett.* **104**, 040502 (2010); J. Alicea, *Phys. Rev. B* **81**, 125318; R. M. Lutchyn, J. D. Sau, and S. Das Sarma, *Phys. Rev. Lett.* **105**, 077001 (2010); Y. Oreg, G. Refael, and F. von Oppen, *Phys. Rev. Lett.* **105**, 177002 (2010).
 - [17] J. D. Sau, S. Tewari, R. M. Lutchyn, T. D. Stanescu, and S. Das Sarma, *Phys. Rev. B* **82**, 214509.
 - [18] L. Fu and C. L. Kane, *Phys. Rev. B* **79**, 161408(R) (2009).
 - [19] V. Mourik, K. Zuo, S. M. Frolov, S. R. Plissard, E. P. A. M. Bakkers, and L. P. Kouwenhoven, *Science* **336**, 1003 (2012); A. Das, Y. Ronen, Y. Most, Y. Oreg, M. Heiblum, H. Shtrikman, arXiv:1205.7073; M. T. Deng, C. L. Yu, G. Y. Huang, M. Larsson, P. Caroff, H. Q. Xu, arXiv:1204.4130.
 - [20] L. P. Rokhinson, X. Liu, J. K. Furdyna, arXiv:1204.4212.
 - [21] J. Liu, A. C. Potter, K. T. Law, P. A. Lee, arXiv:1206.1276
 - [22] J. D. Sau, E. Berg and B. I. Halperin, arXiv:1206.4596
 - [23] I. Buluta and F. Nori, *Science* **326**, 108 (2009).
 - [24] L. Jiang, D. Pekker, J. Alicea, G. Refael, Y. Oreg and F. Von Oppen, *Phys. Rev. Lett.* **107**, 236401 (2011).
 - [25] S. Giorgini, L.P. Pitaevskii, and S. Stringari, *Rev. Mod. Phys.* **80**, 1215 (2008).
 - [26] D. Porras and J. I. Cirac, *Phys. Rev. Lett.* **92**, 207901 (2004).
 - [27] J. Clarke and F.K. Wilhelm, *Nature (London)* **453**, 1031 (2008); J.Q. You and F. Nori, *Nature (London)* **474**, 589 (2011).
 - [28] T. W. B. Kibble, *J. Phys. A* **9**, 1387 (1976); W. H. Zurek, *Nature (London)* **317**, 505 (1985).
 - [29] J. Dziarmaga, *Adv. Phys.* **59**, 1063 (2010); A. Polkovnikov, K. Sengupta, A. Silva, and M. Vengalattore, *Rev. Mod. Phys.* **83**, 863 (2011).
 - [30] J. Dziarmaga and M. M. Rams, *New J. Phys.* **12**, 055007 (2010); J. Dziarmaga, P. Laguna, and W. H. Zurek, *Phys. Rev. Lett.* **82**, 4749 (1999).
 - [31] See Supplemental Material for mathematical details of numerical calculations, energy spectra during two processes, and dynamics of MFs fusion.
 - [32] Our numerical calculations show that two interaction terms like $-i\gamma_1\gamma_2$ or $-i\gamma_3\gamma_4$ have negligibly weak effects.
 - [33] J. Simon, W. Bakr, R. Ma, M. Tai, P. Preiss, and M. Greiner, *Nature (London)* **472**, 307 (2011).
 - [34] J. Sherson, C. Weitenberg, M. Endres, M. Cheneau, I. Bloch, and S. Kuhr, *Nature (London)* **467**, 68 (2010); W. Bakr, A. Peng, M. Tai, R. Ma, J. Simon, J. Gillen, S. Foelling, L. Pollet, and M. Greiner, *Science* **329**, 547 (2010).
 - [35] A. Friedenauer, H. Schmitz, J. Glückert, D. Porras, and T. Schätz, *Nature Phys.* **4**, 757 (2008); R. Islam, E. Edwards, K. Kim, S. Korenblit, C. Noh, H. Carmichael, G. Lin, L. Duan, C. Wang, J. Freericks, et al., *Nature Commun.* **2**, 377 (2011); K. Kim, S. Korenblit, R. Islam, E. Edwards, M. Chang, C. Noh, H. Carmichael, G. Lin, L. Duan, C. J. Wang, et al., *New J. Phys.* **13**, 105003 (2011).
 - [36] J. Britton, B. Sawyer, A. Keith, C. Wang, J. Freericks, H. Uys, M. Biercuk, and J. Bollinger, *Nature (London)* **484**, 489 (2012).
 - [37] C. Rigetti, J.M. Gambetta, S. Poletto, B.L.T. Plourde, J.M. Chow, A.D. Corcoles, J.A. Smolin, S.T. Merkel, J.R. Rozen, G.A. Keefe, M.B. Rothwell, M.B. Ketchen, M. Steffen, *Phys. Rev. B* **86**, 100506(R) (2012).

Supplementary material

ENERGY SPECTRUM

Using a Bogoliubov transformation $a_m^\dagger = \sum_n (u_{nm} c_n^\dagger + v_{nm} c_n)$, Kitaev's wire Hamiltonian

$$H = - \sum_{j=1}^N h_j (2c_j^\dagger c_j - 1) - \sum_{j=1}^{N-1} J (c_j - c_j^\dagger)(c_{j+1} + c_{j+1}^\dagger) \quad (9)$$

can be diagonalized into $H = \sum_m (E_m a_m^\dagger a_m - E_m a_m a_m^\dagger)$, where $E_m < 0$. Due to the particle-hole symmetry, the spectrum has conjugate pairs with negative/positive energy, and we call a_m^\dagger quasiparticle, a_m quasihole. One can obtain the energy spectrum during the two quench processes:

$$\text{Process I: } h_n(t) = \alpha^2 n^2 + h_0 + t/t_Q \quad (10)$$

$$\text{Process II: } h_n(t) = \alpha^2 (n - N/2 - 1/2)^2 + h_0 + t/t_Q$$

The energy spectrum is shown in Fig. 4. One can observe that there is always an energy gap during the quench process, and Majorana zero modes will appear when part of the chain is engineered into topological phase. Especially, for the process II, four Majorana fermions (MFs) will appear.

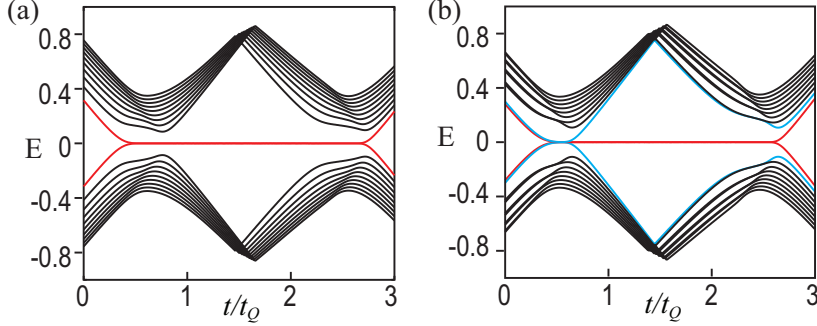


FIG. 4. Energy spectrum of quench process I (a) and II (b). In (a), we take the parameters as $\alpha = 2^{-7}$, $h_0 = -1.8$, $N = 100$, and t/t_Q from 0 to 3. In (b), we take the parameters as $\alpha = 2^{-6}$, $h_0 = -1.7$, $N = 100$, and t/t_Q from 0 to 3. For simplicity, we only plot several states with energy around 0.

NUMBER OF EMERGENT EXCITATIONS

The eigenstate of the system can be constructed by N particles, each of them is chosen from (a_m^\dagger, a_m) conjugate pairs, which reads,

$$|\psi\rangle = \prod_{j \in A} a_j \prod_{i \in N-A} a_i^\dagger |0\rangle / N_0 \quad (11)$$

where N_0 is the normalization constant. To calculate the number of excitations created by the quench process, we start with a groundstate, $|\psi_0\rangle = \prod_i a_i^\dagger |0\rangle / N_0$, evolve the state into $|\psi_f\rangle$, with time-evolution operator $U = T \left\{ \exp \left[-i \int_{t_0}^{t_f} H(t) dt \right] \right\}$:

$$|\psi_f\rangle = U |\psi_0\rangle = U \prod_i a_i^\dagger |0\rangle / N_0 = \prod_i (U a_i^\dagger U^\dagger) |0\rangle \quad (12)$$

Therefore, we can simply calculate the time-evolution of each quasiparticle a_m^\dagger , $a_m^\dagger(t_f) = U a_m^\dagger U^\dagger$. Apparently, the evolved quasiparticle $a_m^\dagger(t_f)$ still satisfy the fermionic commutation relation $\{a_m(t_f), a_n(t_f)\} = \{a_m^\dagger(t_f), a_n^\dagger(t_f)\} = 0$, and $\{a_m^\dagger(t_f), a_n(t_f)\} = \delta_{mn}$.

To implement the time-evolution numerically, one may discretize the time-evolution operator by using the time-slicing procedure:

$$U = T \left\{ \exp \left[-i \int_{t_0}^{t_f} H(t) dt \right] \right\} \approx \prod_t \exp [-iH(t_i)\Delta t] \quad (13)$$

with $\Delta t \ll 1$. It should be noted that it is crucial to retain the unitarity of $\exp [-iH(t_i)\Delta t]$ throughout the calculation:

$$\exp [-iH(t_i)\Delta t] = A \exp(-i\Lambda\Delta t)A^\dagger \quad (14)$$

where $H(t_i) = A\Lambda A^\dagger$, A is a unitary matrix $AA^\dagger = I$ and Λ is a diagonal matrix.

Meanwhile, one can diagonalize the final Hamiltonian $H(t_f)$, obtains Bogoliubov quasiparticles $(b_1^\dagger, \dots, b_N^\dagger)$, and Bogoliubov quasiholes (b_1, \dots, b_N) . The groundstate of the final Hamiltonian is composed with all the quasiparticles $(b_1^\dagger, \dots, b_N^\dagger)$. Therefore, the excitation number in the evolved state $|\psi_f\rangle$ is $n_{ex} = \sum_i \langle \psi_f | b_i b_i^\dagger | \psi_f \rangle$. We may rewrite b_n as superposition of $a_m^\dagger(t_f)$ and $a_m(t_f)$:

$$b_n^\dagger = \sum_m [\beta_{nm}^* a_m^\dagger(t_f) + \eta_{nm} a_m(t_f)]. \quad (15)$$

The excitation number can be written as

$$n_{ex} = \sum_{n,m} |\eta_{nm}|^2 \quad (16)$$

EXCITATIONS IN TIM

To measure the fused excitations in TIM unambiguously, we may either tune the magnetic field h_i or the spin-spin coupling J to 0. One can measure the spin-spin correlation $\langle \sigma_i^x \sigma_{i+1}^x \rangle = \langle (c_j - c_j^\dagger)(c_{j+1} + c_{j+1}^\dagger) \rangle$ at $h_i = 0$ to study the domain wall excitations, as shown in Fig. 5(a). Similarly, one can measure the magnetization $\langle \sigma_i^z \rangle = \langle 2c_i^\dagger c_i - 1 \rangle$ when $J = 0$ to witness the flipped spin excitations, as shown in Fig. 5(b)-(c). It clearly shows for the quench process II, either the domain wall excitations (Fig. 5(a)) or the flipped spin excitations (Fig. 5(b)) are not localized well. On the contrary, for the quench process III introduced in the paper, where the MFs are fused at the edge of the chain and may result in the prefect trapping of the fused excitation, as plotted in Fig. 5(c).

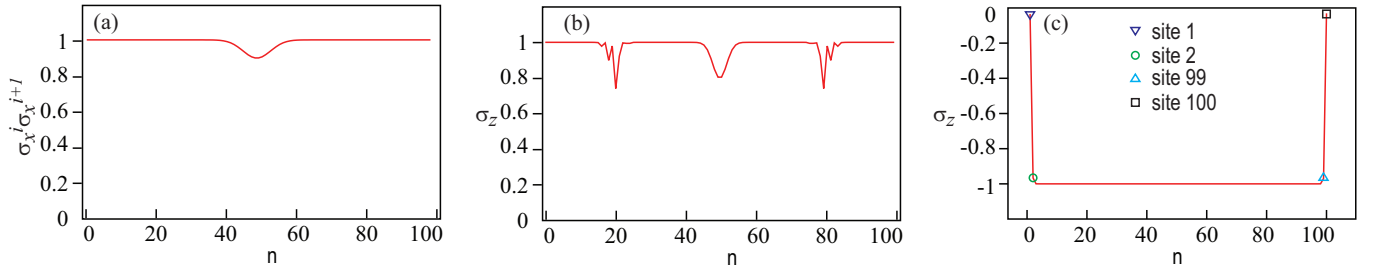


FIG. 5. (a)-(b) Spatial distribution of the domain wall and flipped spin excitations in quench process II. (c) Spatial distribution of the flipped spin excitations in quench process III.

TUNNELING OF UNPAIRED MFS

We numerically calculate the cases where two unpaired MFs are approaching, and study how the wave packets behave. More specifically, as proposed in this paper, we use quench process II to create two pairs of MFs (γ_1, γ_2) and (γ_3, γ_4) , and bring two unpaired MFs (γ_2, γ_3) close to each other at the center. Then we pause the changing of potential, and let it evolve under that situation for certain time duration t_e . The numerical results are shown in Fig. 6. It clearly shows that finite tunneling appears between the two unpaired MFs (γ_2, γ_3) and the tunneling exhibits oscillating behaviors:

$$\tilde{\gamma}_2 = \cos[2A(l)t_e]\gamma_2 + \sin[2A(l)t_e]\gamma_3, \quad \tilde{\gamma}_3 = \cos[2A(l)t_e]\gamma_3 - \sin[2A(l)t_e]\gamma_2 \quad (17)$$

where $A(l)$ is the coupling strength of γ_2 and γ_3 .

It can also be observed that the MFs (γ_1, γ_4) at both ends are very localized, and shows no time evolution. All these facts suggest that the interaction terms like $-i\gamma_1\gamma_2$ or $-i\gamma_3\gamma_4$ are negligibly small which we can safely ignore.

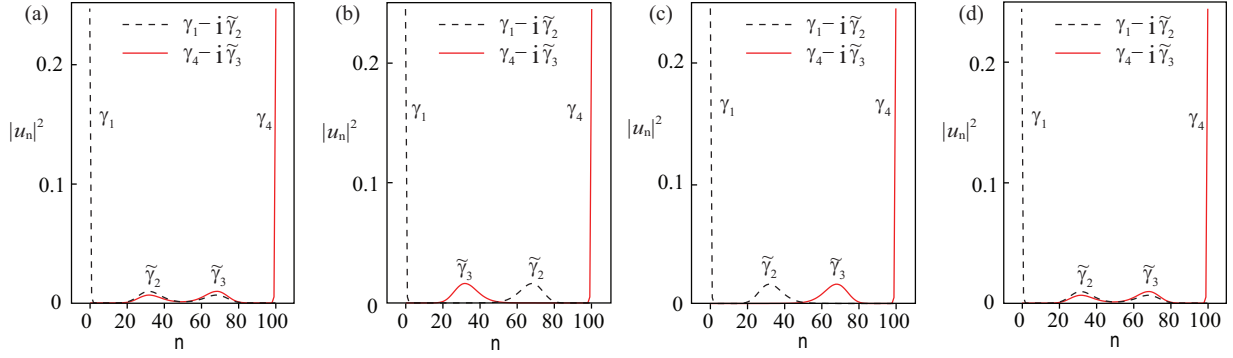


FIG. 6. Time evolution of the wave packets of four MFs. Here we choose $\alpha = 0.02$, $J = 1$, $N = 100$ and γ_2 is separated by $l = 35$ lattice spacing with γ_3 . In (a)-(d), we choose the time duration t_e to be 100, 300, 671, 1586. Here the period of oscillation is $\pi/A(l) \approx 1486$.